ORIGINAL PAPER

CrossMark

The numerical study of the effect of design parameters on EWOD actuation in microchannels of rectangular cross section

Sajad Pooyan[1] · Mohammad Passandideh-Fard[1]

Abstract

Electrowetting on Dielectric (EWOD) method is widely used to actuate microdroplets sandwiched between parallel plates in microfluidic chips. However, utilization of this method to transport liquid plugs in conduits has not been comprehensively studied to date. In this paper, the EWOD actuation of a liquid plug confined in a microchannel of rectangular cross section is numerically studied using OpenFoam. The effect of various parameters including electrowetting dimensionless number (η), contact angle hysteresis (CAH), dynamic viscosity and surface tension coefficient on transport velocity is investigated by employing an interactive simulation approach. The transport velocity can be considered a gauge to evaluate the actuation efficiency. The results show that, increasing η has a greater impact on velocity for larger values of CAH. In addition, it is shown that the average velocity increases linearly by increasing the surface tension coefficient. An inverse relationship between velocity and dynamic viscosity is also observed. These trends are in accordance with the theoretical model developed for a similar case in the literature. To estimate the maximum possible gap size between electrodes (MPGS), non-actuated distance travelled before the liquid plug comes to stop is evaluated. The results show that by decreasing the values of η, the effect of changing CAH on MPGS becomes more substantial.

Keywords EWOD · Microchannel · Liquid plug · InterFoam · Simulation

1 Introduction

Microfluidics is a technology in which small quantities of fluids (in the range of microliter to picoliter) are transported and manipulated through channels of micrometer scale integrated in a microfluidic chip. The motivation for the application of microfluidics is the need to manipulate tiny amounts of samples/reagents or fabricate portable test devices involving liquid processing. As examples, chemical microreactors, devices to detect a biologic entity in a small amount of sample or point-of-care medical test devices. Today, microfluidic devices, which are also commonly referred to as Labs-on-a-Chip (LOC), are of high importance to many biotechnology, chemistry and engineering applications due to their superior

characteristics such as low material and energy consumption, low response times and high accuracy.

One newly emerging subcategory of microfluidics is "droplet microfluidics", also called droplet-based microfluidics. Working with tiny quantities of liquid, which form a microdroplet or a liquid plug in a microchannel, instead of continuous flows, dramatically decreases the amount of required samples/reagents and enables these devices to perform complicated fluidic operations more efficiently.

One of the most innovative and successful methods to actuate and manipulate microdroplets in droplet-based systems is Electrowetting on dielectric (EWOD). In this method, applying an electric field near the line of contact of a droplet and a solid surface, exerts an electrostatic force to the droplet free surface and propels the droplet in the direction of the force. The electric field is generated by electrifying a metallic plate, called electrode, covered with a thin dielectric layer, underneath the droplet meniscus. The consequent effect of the electrostatic force exerted on the free surface is decreasing the contact angle in the portion of the contact line located on the electrode. If the static equilibrium contact angle is θ_0, contact angle after applying the electric potential, θ_v, will

✉ Mohammad Passandideh-Fard
mpfard@um.ac.ir

Sajad Pooyan
sajad.pooyan@mail.um.ac.ir

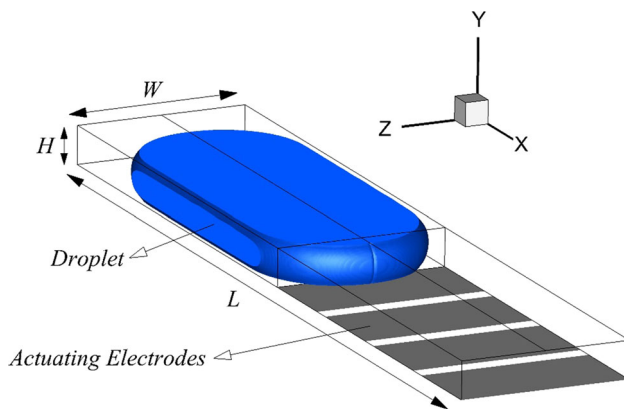[1] Department of Mechanical Engineering, Ferdowsi University of Mashhad, Mashhad, Iran

Fig. 1 The overall view of the solution domain

have a smaller value and can be calculated using Young–Lippmann equation as follows:

$$\cos\theta_V = \cos\theta_0 + \eta \tag{1}$$

where, η is called electrowetting dimensionless number. This number indicates the relative importance of the surface energy due to electrostatic force (electrowetting phenomenon) comparing to the surface energy associated with surface tension and can be calculated by following relation [1]:

$$\eta = \frac{\varepsilon_0 \varepsilon_d}{2\sigma d} V^2 \tag{2}$$

In above relation, σ, ε_0, ε_d and d are surface tension coefficient, the electric permittivity of vacuum ($\varepsilon_0 = 8.85 \times 10^{-12} \frac{F}{m}$), relative electric permittivity of the dielectric layer and the thickness of dielectric layer. V is the voltage applied to the actuating electrode.

To transport the droplet between two points, an array of individually controllable electrodes are placed between those points (Fig. 1). As shown in Fig. 2, if electric potential is applied to the electrode that sits under the meniscus of the droplet, the contact angle on that electrode decreases from equilibrium value, θ_0, to the actuated value, θ_v. The difference between the contact angles at the two sides causes the
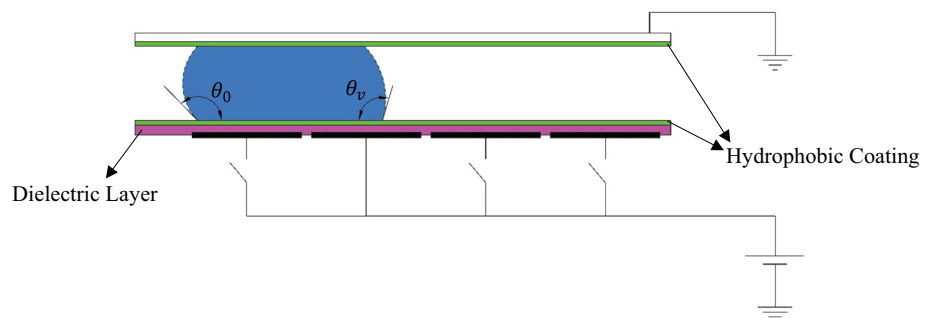
drop to travel towards the active electrode. The droplet can be transported on the array of electrodes by sequentially activating the electrodes in a direction. It should be noted that the prerequisite for the possibility of this method is hydrophobicity of the surfaces in contact with droplet, i.e. the contact angle before applying a voltage should be larger than 90°. For this reason, the solid surfaces in contact with droplet are coated with a hydrophobic material.

Many researchers has studied the application of EWOD method to transport circular droplets confined between two horizontal parallel plates. For instance, Yamamoto et al. [2] numerically and theoretically investigated the effect of various parameters including applied voltage, droplet diameter and geometric design parameters on the shape evolution and transport velocity of a circular drop sandwiched between parallel plates.

Although EWOD actuation of circular droplets confined between parallel plates is very common and the systems based on this design are widely used, utilization of the EWOD method to transport liquid plugs confined in microchannels is not as prevalent. However, transporting liquid plugs in microchannels is needed in many microdevices [3]. As examples, the systems in which particles like cells encapsulated in small liquid plugs are transferred through microfluidic circuits [4] and devices that deliver controlled tiny amounts of medicine to patient body [5]. Therefore, EWOD method can be introduced as a reliable and efficient method to transport liquid plugs in microchannels.

The idea of using the EWOD method to actuate fully confined liquid plugs was introduced by Kedzierski et al. [6]. They designed a micropump in which liquid plugs, confined in microchannels of rectangular cross section, act as pistons and pump another fluid. Despite relatively low power consumption, their pump could generate up to 2.5 kpa. Later, it was shown that by actuating multiple liquid plugs in series in a microchannel, larger pressure differences can be generated [7].

Shabani and Cho [8] utilized EWOD method in another device. In their design, a droplet sitting on the surface of a microfluidic chip at the entrance of a channel could be sucked into a rectangular microchannel by actuating the meniscus of

Fig. 2 The overview of the electrowetting on dielectric method

the liquid column in the microchannel. They also studied the effect of parameters including applied voltage and contact angle of the sessile droplet on suction rate [9].

In an innovative device, Kedzierski et al. [10] actuated the liquid plugs in microchannels of circular cross section. They integrated several of these microchannels in one microfluidic chip, to pump a larger volume of liquid. The liquid flow was directed to a mechanical arm to show that the fabricated device has the potential to activate a microrobot. The required electric power, voltage, the generated flow rate, pressure and mechanical power were investigated. In addition, the device was successfully operated in reverse manner to harvest electrical energy from an available source of mechanical energy by employing the "reverse electrowetting" concept.

As detailed above, the EWOD actuation of liquid plugs in microchannels potentially has significant applications in various fields of microfluidics. Therefore, interactive simulation can be helpful in designing innovative systems based on this technique and provide a general insight about its capabilities and limitations. In this study, the actuation of liquid plugs confined in microchannels of rectangular cross section is numerically simulated and the effect of important design parameters including electrowetting dimensionless number, contact angle hysteresis, liquid viscosity and surface tension coefficient on transport velocity are studied. The interactive simulation approach followed in this paper provides a learning process about the behaviour of the system in response to alteration of design parameters. In other words, by comparison of the results of multiple simulation cases, the relationships between various design parameters and dependant variable (i.e. transport velocity) can be modeled. By knowing these relationships, a designer can design an optimized system or an operator can predict the response of a fabricated chip to alteration of each parameter.

It is worth mentioning that, the devices in which circular droplets are sandwiched between parallel plates have been studied in numerous research works from various standpoints. However, the results of those works cannot be generalized to include the systems with fully confined liquid plugs. The reason is the difference between the shape of a circular droplet and a liquid plug and their interactions with channel walls, this makes their internal flows and shear forces on surfaces different.

2 Numerical method

To perform the numerical simulation in this study, InterFoam solver is used. InterFoam is one of the solvers available in OpenFoam, an open-source numerical simulation package. This solver uses the Volume of Fluid (VOF) technique to simulate the flows with free surface. VOF is one of the most powerful techniques for free surface tracking and reconstruc-

tion. This technique is widely utilized to predict the fluid behaviour, when there is free surface with considerable surface tension in complex geometries, for example droplet formation and transport, bubble formation and sprays.

2.1 Governing equations and VOF formulation

The main equations governing the fluid flow are continuity and momentum equations for incompressible flow with constant properties:

$$\vec{\nabla} \cdot \vec{V} = 0 \tag{3}$$

$$\frac{\partial \vec{V}}{\partial t} + \vec{\nabla} \cdot \left(\vec{V} \vec{V} \right) = -\frac{1}{\rho} \vec{\nabla}_p + \frac{1}{\rho} \vec{\nabla} \cdot \overset{\leftrightarrow}{\tau} + \vec{g} + \frac{1}{\rho} \vec{F}_b \tag{4}$$

where $\vec{V}$ is the velocity, p the pressure, ρ the density, $\vec{g}$ the gravitational acceleration $\vec{F}_b$ the body force per unit volume and $\overset{\leftrightarrow}{\tau}$ the stress tensor. The stress tensor is correlated with velocity through the rate of strain tensor as follows:

$$\overset{\leftrightarrow}{\tau} = 2\mu \overset{\leftrightarrow}{z} \tag{5}$$

$$\overset{\leftrightarrow}{z} = \frac{1}{2} \left[\left(\vec{\nabla} \vec{V} \right) + \left(\vec{\nabla} \vec{V} \right)^T \right] \tag{6}$$

where μ is the dynamic viscosity.

Surface tension causes a pressure jump across the free surface, assuming the surface tension coefficient of the liquid to be constant, the value of this pressure jump can be calculated as:

$$p_s \equiv (p_l - p_v) = \sigma \kappa \tag{7}$$

p_l is the pressure inside the liquid, p_v is the pressure outside the liquid and κ is the curvature of the free surface. In InterFoam, the surface tension effect is modeled using the continuum surface force (CSF) method [11]. In this method, the surface tension force is included as an additional body force source term in momentum equation (Eq. 4) in cells on or adjacent to the free surface. The curvature of the free surface, κ, is obtained by following relations:

$$\kappa = -\left(\vec{\nabla} \cdot \vec{\hat{n}} \right), \quad \vec{\hat{n}} = \frac{\vec{n}}{|\vec{n}|} \tag{8}$$

where $\vec{n}$ is the normal vector to the free surface pointing to inside the liquid phase.

As mentioned above, the VOF technique is used to track the free surface. In this technique, a numerical parameter called volume fraction, f, is defined as follows:

$$f = \frac{Volume\ of\ the\ cell\ filled\ with\ liquid\ phase}{Total\ volume\ of\ the\ cell} \tag{9}$$

With above definition, the value of the parameter f for any cell indicates whether the cell is in liquid phase, on free surface or outside the liquid phase:

$$f(x,t) = \begin{cases} 1 & inside\ liquid\ phase \\ 0 < f < 1 & on\ free\ surface \\ 0 & outside\ liquid\ phase \end{cases} \quad (10)$$

Concerning Eq. 8, normal vectors to free surface are required to calculate the curvature of the free surface. This vectors are calculated using the parameter f:

$$\vec{n} = \vec{\nabla} f \quad (11)$$

Besides, the physical properties, e.g. viscosity and density, in each cell are determined using volume fraction weighted average of the properties of the two phases:

$$\rho = f \rho_l + (1 - f) \rho_{Air} \quad (12)$$
$$\mu = f \mu_l + (1 - f) \mu_{Air} \quad (13)$$

where, l subscript denotes the liquid phase and Air subscript denotes the surrounding air phase.

In InterFoam, the conservation advection equation for the volume fraction is in the following form:

$$\frac{\partial f}{\partial t} + \nabla \cdot \left(\vec{V} f \right) - \nabla \cdot \left(f (1 - f) \vec{U}_r \right) = 0 \quad (14)$$

In Eq. 14, $\vec{U}_r$ is an artificial "interface-compression velocity" defined in the vicinity of the interface so that the local flow steepens the gradient of the volume fraction function and the interface resolution is improved. $\vec{U}_r$ is given by:

$$U_r = \min \left[C_f \frac{|\phi|}{|S_f|}, \max \frac{|\phi|}{|S_f|} \right] \hat{\vec{n}}_f \quad (15)$$

where $\hat{\vec{n}}_f$ is the normal vector of the cell surface, ϕ is the mass flux, S_f is the cell surface area and C_f is an adjustable coefficient by which the intensity of compression is controlled [12]. There is no compression if C_f is set to zero, a conservative compression for $C_f = 1$, and high compression if $C_f > 1$.

Above mentioned equations are solved based on the PIMPLE algorithm, after discretization in three dimensions. As the equations are solved transient in time, the value of time step is automatically set by the software to maintain the maximum courant number below 1. Table 1 shows the values chosen for InterFoam adjustable numerical parameters. The discretization schemes employed for the terms of the governing equations are the InterFoam default schemes presented in its tutorial problem for laminar capillary flow.

Table 1 Selected values for the InterFoam numerical parameters

Parameter	Value	Notes
C_f	1	Interface-compression intensity coefficient
$N_{f\text{-}corr}$	2	Number of volume fraction corrector steps
$N_{f\text{-}subcycles}$	1	Number of volume fraction subcycles
$N_{nonortho\text{-}corr}$	0	Only used for nonorthogonal meshes
N_{corr}	3	Maximum number of PISO loops
momentumPredictor	No	Momentum prediction step

2.2 Geometry of solution domain and boundary conditions

As displayed in Fig. 1, the solution domain is a microchannel of rectangular cross section with height h, width w and length L which is assumed open to ambient air at the two ends. The liquid plug occupies a part of the channel length and the remaining space is filled with air. To reduce the undesired oscillations around the equilibrium shape at the beginning of solution, the initial shape of the liquid plug is defined as close as possible to the equilibrium shape of a stationary plug.

The velocity and pressure boundary conditions on channel walls are "fixedValue" and "fixedFluxPressure", respectively.[1] By using these conditions, all the velocity components on walls are set to zero and the pressure gradient is adjusted so that the boundary flux matches the zero velocity boundary condition considering body forces such as gravity and surface tension. For the two ends of the channel which are free to atmosphere, the Combination of "pressureInletOutletVelocity" and "totalPressure" boundary conditions are used for pressure and velocity, respectively. This combination permits both outflow and inflow according to the internal flow while maintaining stability [13]. The "totalPressure" condition sets the value of relative pressure to zero for outward flows and sets it to $-\frac{1}{2}\left|\vec{V}^2\right|$ for inward flows. pressureInletOutletVelocity condition applies zero gradient on all velocity components except for the tangential component of inward flows for which the value is set to zero.

The contact angles are boundary conditions for volume fraction solution and should be predefined. The effect of contact angle hysteresis (CAH) on results is also considered in this work. When contact line is advancing on a solid surface,

---

[1] The names used for the boundary conditions are identical to names used to specify them in the computer program.

Table 2 Details of the mesh used to study mesh independence

Number of cells in:	Coarse mesh	Medium mesh	Fine mesh
Channel length ($L = 6$ mm)	300	600	900
Half of channel width ($W/2 = 0.5$ mm)	25	50	75
Channel height ($H = 0.22$ mm)	11	22	33
Total number of cells	82,500	660,000	2,227,500

contact angle is larger than its static equilibrium value and when the contact line is receding, contact angle is smaller than the static equilibrium value. Contact angle hysteresis, defined as the difference between the values of advancing and receding contact angles, depends on the properties of solid surface and liquid and usually has non-zero value. To include the effect of CAH in simulations, the static value plus half of the CAH value is specified as the contact angle for surfaces on which liquid plug leading meniscus moves, and inversely, the static value minus half of the CAH value is specified as the contact angle for surfaces on which liquid plug trailing meniscus moves. Contact angle on actuating electrodes is set to θ_V (Fig. 2). In this study the value of θ_V is calculated by Eq. 1. The dependence of the value of contact angles on the magnitude of the velocity of contact line is assumed negligible. The validity of this assumption has been verified in [14].

Regarding the symmetry of the solution domain and boundary conditions around the x–y plane and the symmetry observed in results of experiments in literature, equations are solved for half of the domain to decrease the computational costs.

2.3 Grid independence verification

The solution is performed using three-dimensional uniform structured mesh generated by Blockmesh, an internal mesh generator of OpenFOAM. Meshing the solution domain with uniform hexahedral cells simplifies the solution of differential equations and enhances the stability. To achieve a mesh independent solution, the actuation of a $0.5\,\mu$l water droplet in a microchannel is simulated using three different mesh sizes. The specifications of the mesh and the domain are mentioned in Table 2.

The position of the leading meniscus of the water plug on the X axis, along the channel length, is plotted versus time in Fig. 3. The origin of the X axis is coincident with the beginning of the first actuating electrode. It is observed that, when the size of cells is 10 µm or lower (i.e. for medium and fine mesh), a mesh independent solution is obtained. Therefore, in all the subsequent simulations, the number of cells are adjusted so that cell size is equal to 10 µm.
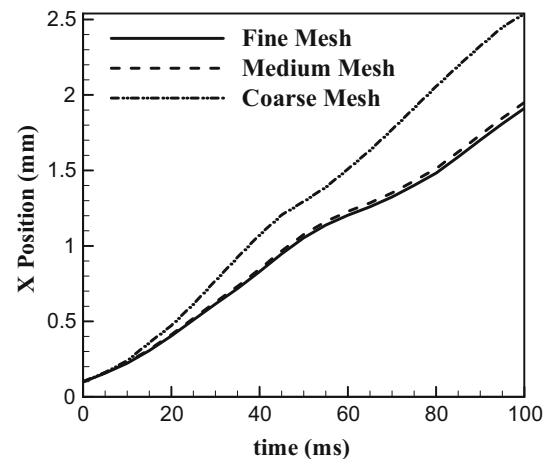

Fig. 3 Mesh independence assessment, the x position of the leading meniscus of a $0.5\,\mu$l water plug versus time is compared using fine, medium and coarse mesh, refer to Table 2 for mesh size details

3 Validation

To validate the numerical solution, simulation results are compared with experimental pictures presented by Pooyan and Passandideh-Fard [14]. In this case, the transport of a 3.64 mercury plug in a microchannel of $W = 2$ mm and $H = 440\,\mu$m is simulated. The electrowetting dimensionless number in experiments has been 0.11 and all the contact angles were measured by image processing and reported. The same contact angles and fluid properties as reported in [14] are used for the simulations. Figure 4 shows the 3D images of the plug moving in the microchannel and Fig. 5 compares these images with images from experiments. Acceptable agreement with experimental images is observed in Fig. 5. In addition, average velocity of the liquid plug in experiment is reported to be 10.8 mm/s whereas the simulation yields 11.8 mm/s. 9% difference between the two velocities confirms the accuracy of simulation results.

4 Results and discussions

4.1 Effect of electrowetting dimensionless number

As mentioned before, electrowetting dimensionless number, η is a measure of the relative intensity of the electrostatic
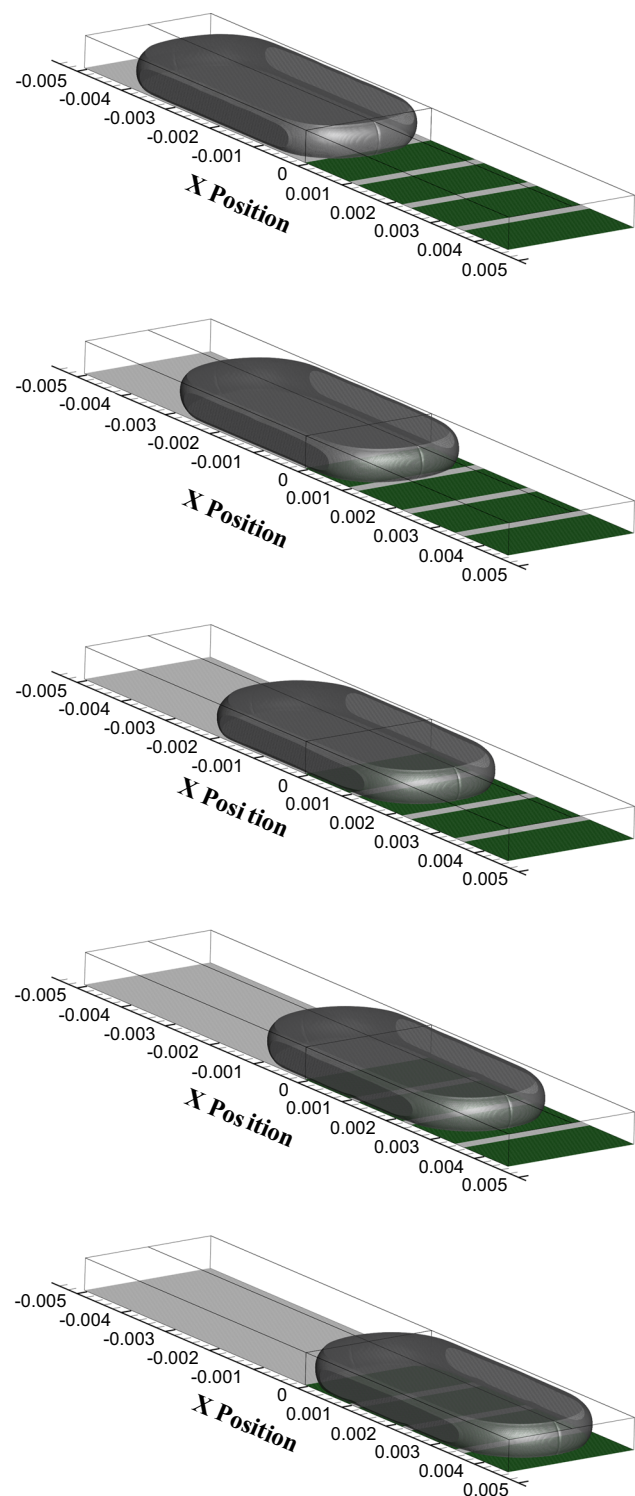
Fig. 4 Time-lapse 3D view of the displacement of a 3.68 μl mercury slug in a microchannel of 2 mm width and 440 μm height, Electrowetting dimensionless number is 0.11, time interval between each two frames is 0.09 s

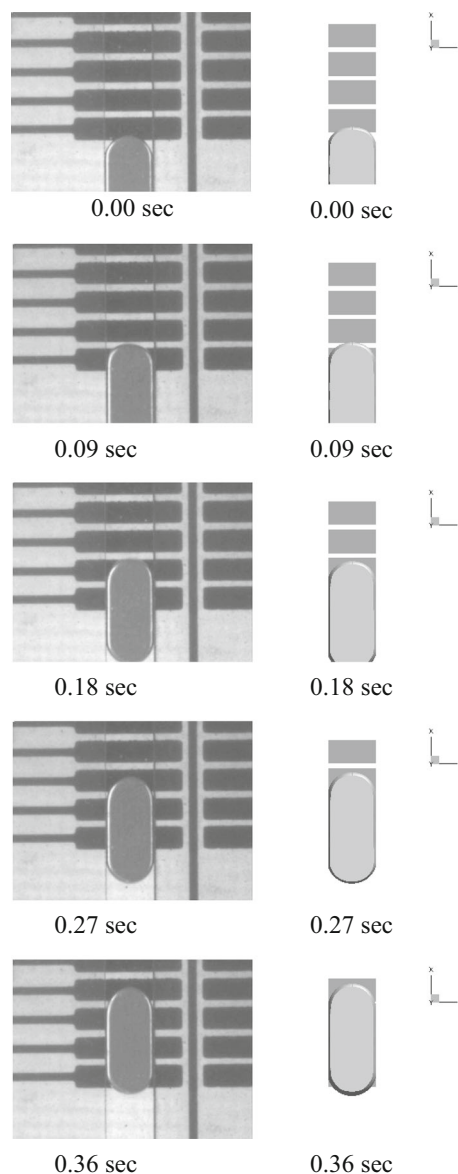**Fig. 5** Comparison between experimental and simulation results, displacement of a 3.68 μl mercury slug in a microchannel of 2 mm width and 440 μm height, Electrowetting dimensionless number is 0.11

actuating force exerted on the free surface compared to the surface tension force. The consequent effect of actuation is to reduce the contact angle in the portion of contact line that

is on the active electrode. Therefore, larger η leads to a larger reduction of contact angle, which in turn, results in a more intense propulsion. Since in most cases aqueous solutions are working liquids in microfluidic platforms, simulations are performed using the properties of pure water. In addition, contact angle hysteresis (CAH) plays an important role in efficiency of transport. Therefore, to account for the effect of CAH, the reported values for the contact angle hysteresis of water on TeflonAF and Cytop are employed in simulations [15–17]. TeflonAF and Cytop are two hydrophobic fluoropolymers extensively used to hydrophobize the EWOD based microfluidic chips and all the channel surfaces are coated with one of these materials. As it is observed that CAH

Table 3 Values of parameters used in simulations

Parameter name	Unit	Value
Density (water)	Kg/m^3	1000
Surface tension coefficient (water)	mN/m	73
Dynamic viscosity (water)	mPa.s	1.0035
Density (air)	mPa.s	0.0148
Dynamic viscosity (air)	Kg/m^3	1
Plug Volume	μl	1
Channel height	μm	250
Channel width	μm	1000
Static Equilibrium contact angle[a]	deg.	105°–115°
Contact angle hysteresis[b]	deg.	8°–12°
Length of each electrode	mm	1.0
Gap between electrodes	mm	0.1

[a] Abbreviated to "CA" in figures

[b] Abbreviated to "CAH" in figures

is lower on surfaces with higher static equilibrium contact angle, three combinations of equilibrium contact angle(CA) and CAH are considered in simulations: CA = 115° and CAH = 8°, CA = 110° and CAH = 10°, CA = 105° and CAH = 12°. The values of parameters used in simulations are listed in Table 3.

Figure 6 shows the position of the leading meniscus of a water plug versus time at different η values and for various contact angles and CAH. The hatched area between x = 1 mm and x = 1.1 mm is the gap between the two adjacent electrodes on which no actuation exists. To perform the simulations, the value of θ_V as a function of η is calculated by Eq. 1. To obtain the average velocity of the plug for each case, the total distance travelled by plug leading meniscus is divided by the elapsed time. The travelled distance is the same for all cases and equal to 2 mm (from starting point at 0.1 mm passed the beginning of the first actuating electrode to the end of second actuating electrode).

Based on results displayed in Fig. 6, increasing η has a greater impact on transport velocity when CAH is larger. Results show that, changing η from 0.4 to 1 when CAH is 8°, rises the average velocity by 312%, whereas for CAH = 12°, average velocity is boosted 534% when η is increased from 0.4 to 1. In other words, changing CAH affects the transport velocity more substantially when η is smaller. For instance, increasing CAH from 8° to 12° when $\eta = 1$, leads to 11% reduction in average velocity whereas when $\eta = 0.4$, it reduces the velocity by 34%. To explain the reason, it should be noted that there are two different factors resisting plug motion, one is the capillary force associated with CAH and the second is the viscous drag forces exerted on plug by channel walls. When η is low, the plug velocity is low, therefore,
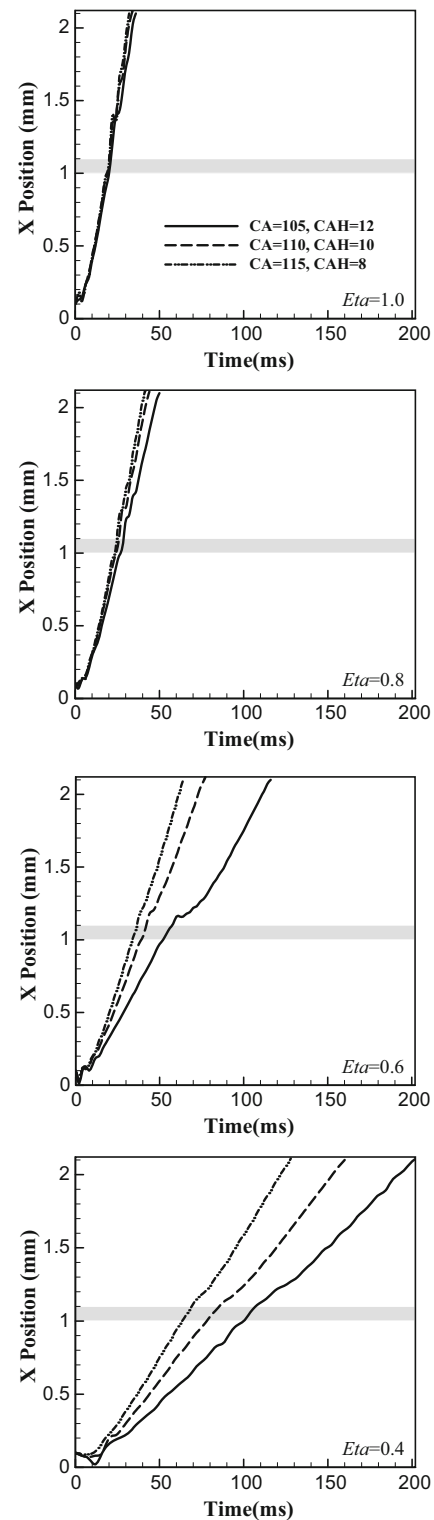

Fig. 6 Position of plug leading meniscus during actuation for various electrowetting dimensionless numbers, the legend of all graphs are similar to the first graph

capillary forces are the dominant resistant effect. By increasing η, as plug velocity increases, viscous dissipation inside the bulk of the liquid and consequently viscous drag forces

increase and become the dominant factor resisting against velocity.

4.2 Maximum possible electrode spacing

A crucial factor in designing microfluidic chips based on EWOD method is the maximum possible distance between two adjacent electrodes. Generally, the accuracy of fabrication equipment limits the minimum achievable gap between electrodes in fabricated chips. On the other hand, if the gaps between electrodes are larger than specific amounts, the plug may experience a substantial velocity reduction when the leading meniscus is travelling on the gap between electrodes or even fail to reach the next electrode. By examining the data presented in Fig. 6, it is observed that there is not a considerable velocity decrease when the plug passes the gap between electrodes. This is because gap size is well below the maximum possible gap size (gap size is 100 μm for the cases shown in Fig. 6). To further evaluate the maximum possible gap size for the actuation of liquid plugs in microchannels, a scenario is simulated in which only the first electrode is active and there is no actuation on subsequent electrodes. Under these conditions, after leading meniscus reaches the end of active electrode, the plug starts to slow down until it eventually stops. The distance between the point where plug leading meniscus stops and the end of active electrode can be considered as a measure of the maximum possible gap size, because if the leading meniscus reaches the next active electrode before coming to stop, it will continue to move on. Maximum Possible Gap Size (MPGS) for various electrowetting dimensionless numbers and different contact angle hysteresis values are displayed in Fig. 7 . As shown in Fig. 7, for higher values of η, plug can travel farther without actuation because of its larger momentum. On the other
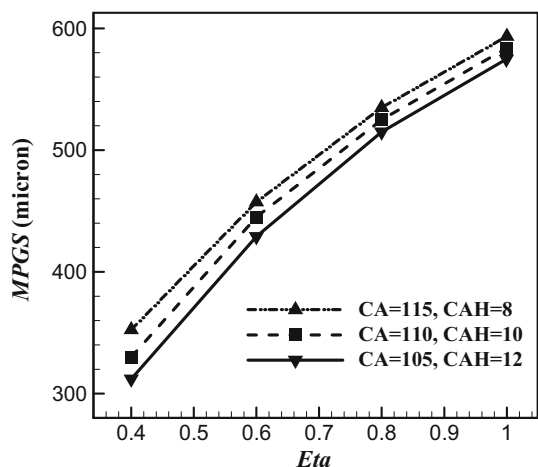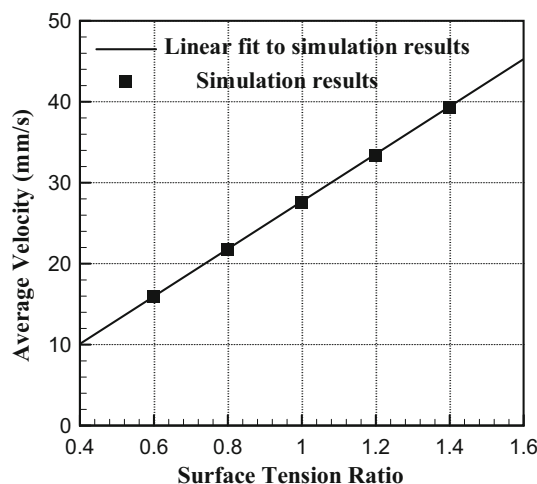

Fig. 8 Average velocity for various surface tension coefficient ratios relative to water for $\eta = 0.6$, CA $= 110°$ and CAH $= 10°$

hand, capillary forces associated with CAH and viscous drag forces are the two factors resisting plug motion. As mentioned before, capillary force is dominant when η is low, and viscous forces are dominant when η is high. As a result, as observed in Fig. 7, increasing the CAH has a greater effect on MPGS when η is lower. As per simulation results, when $\eta = 0.4$, increasing the CAH value from 8° to 12°, decreases the MPGS by 11.3%, whereas, for $\eta = 1$, MPGS is decreased 3.2% by increasing CAH from 8° to 12°.

4.3 Effect of surface tension coefficient

Microfluidic systems are designed to handle various aqueous solutions with different surface tension coefficients. The effect of surface tension coefficient on the average velocity of a liquid plug is studied in this section. The average velocity of the plug for different values of surface tension coefficient are displayed in Fig. 8. The surface tension coefficient values are shown as multipliers of pure water surface tension coefficient. As observed in Fig. 8, increasing the surface tension coefficient leads to higher velocities. Moreover, this figure shows a linear relationship between the velocity and surface tension coefficient. This linear relationship is also proposed by the theoretical model for EWOD actuation of liquid plugs in rectangular microchannel developed by Pooyan and Passandideh-Fard [14].

4.4 Effect of dynamic viscosity

The effect of changing dynamic viscosity on average velocity is shown in Figure 9. Dynamic viscosity values are represented by multipliers of pure water dynamic viscosity. The curve best fitting the simulation results indicates an inverse relationship between average velocity and viscosity.
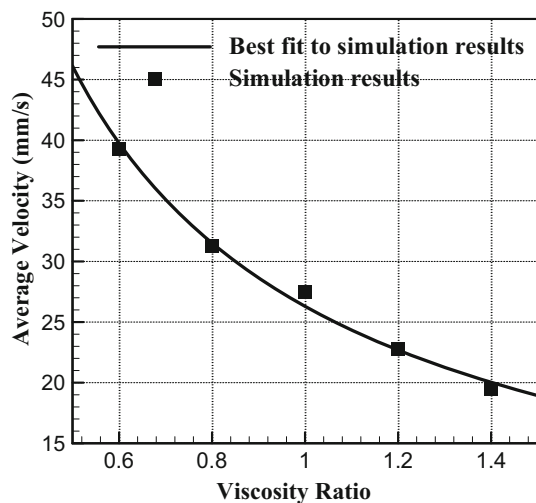

Fig. 7 Maximum possible gap size (MPGS) versus electrowetting dimensionless number (η)

Fig. 9 Average velocity for various dynamic viscosity ratios relative to water for $\eta = 0.6$, CA = 110° and CAH = 10°

As observed in Fig. 9, the slope of the fitted curve decreases with increasing the viscosity. This trend is also in accordance with the theoretical model presented in [14]. It should be noted that, by increasing the viscosity, the assumption regarding the independence of contact angles and the velocity of contact line, which is used in this work, will not be accurate [18]. Therefore, the curve should not be extrapolated for larger values of viscosity.

5 Conclusions

In this study, we used OpenFoam numerical modeling package to simulate the transport of a liquid plug confined in a rectangular microchannel by means of the EWOD method. In this method, the contact angle of a liquid plug is reduced asymmetrically by applying electrostatic force to the free surface of the plug in the vicinity of the contact line and the difference between the contact angles at the two menisci provides the driving force to move the plug. The effect of important parameters including electrowetting dimensionless number, contact angle hysteresis, liquid surface tension coefficient and viscosity on transport velocity were investigated. The key difference distinguishing this work is the shape of microchannel in which the liquid is actuated.

Notable findings of this research are as listed below:

1. Increasing η has a greater impact on transport velocity when CAH is larger. Results show that, changing η from 0.4 to 1 when CAH is 8°, rises the average velocity by 312%, whereas for CAH = 12°, average velocity is boosted 534% when η is increased from 0.4 to 1.
2. Maximum possible gap size (MPGS) for various values of CAH and electrowetting dimensionless number is

obtained by measuring the unactuated distance travelled before plug stops. Simulations showed that increasing the CAH has a greater effect on MPGS when η is low. As per simulation results, when $\eta = 0.4$, increasing the CAH value from 8° to 12°, decreases the MPGS by 11.3%, whereas, for $\eta = 1$, MPGS is decreased 3.2% by increasing CAH from 8° to 12°.
3. Increasing the value of surface tension coefficient was proved to boost the average velocity and a linear relationship between the velocity and surface tension coefficient was observed which is in accordance with the theoretical model developed in previous works.
4. Simulation results demonstrated an inverse relationship between dynamic viscosity of the liquid and velocity which is also in agreement with the theoretical model presented in the literature.

References

1. Frieder, M., Jean-Christophe, B.: Electrowetting: from basics to applications. J. Phys. Condens. Matter **17**(28), R705 (2005)
2. Yamamoto, Y., Ito, T., Wakimoto, T., Katoh, K.: Numerical and theoretical analyses of the dynamics of droplets driven by electrowetting on dielectric in a Hele-Shaw cell. J. Fluid Mech. **839**, 468–488 (2018)
3. Mashaghi, S., Abbaspourrad, A., Weitz, D.A., van Oijen, A.M.: Droplet microfluidics: a tool for biology, chemistry and nanotechnology. TrAC Trends Anal. Chem. **82**, 118–125 (2016)
4. Shang, L., Cheng, Y., Zhao, Y.: Emerging droplet microfluidics. Chem. Rev. **117**(12), 7964–8040 (2017)
5. Damiati, S., Kompella, U.B., Damiati, S.A., Kodzius, R.: Microfluidic devices for drug delivery systems and drug screening. Genes **9**(2), 103 (2018)
6. Kedzierski, J., Berry, S., Abedian, B.: New generation of digital microfluidic devices. J. Microelectromech. Syst. **18**(4), 845–851 (2009)
7. Jenkins,J., Kim, C.: Generation of pressure by EWOD-actuated droplets. In: Presented at the Solid-State Sensors, Actuators, and Microsystems Workshop Hilton Head Island, South Carolina, June 3–7, 2012 (2012)
8. Shabani, R., Cho, H.J.: Active surface tension driven micropump using droplet/meniscus pressure gradient. Sens. Actuators B Chem. **180**, 114–121 (2013)
9. Shabani, R., Cho, H.J.: Flow rate analysis of an EWOD-based device: How important are wetting-line pinning and velocity effects? Microfluid. Nanofluid. **15**(5), 587–597 (2013)
10. Kedzierski, J., Meng, K., Thorsen, T., Cabrera, R., Berry, S.: Microhydraulic electrowetting actuators. J. Microelectromech. Syst. **25**(2), 394–400 (2016)
11. Brackbill, J., Kothe, D.B., Zemach, C.: A continuum method for modeling surface tension. J. Comput. Phys. **100**(2), 335–354 (1992)
12. Hoang, D.A., van Steijn, V., Portela, L.M., Kreutzer, M.T., Kleijn, C.R.: Benchmark numerical simulations of segmented two-phase flows in microchannels using the volume of fluid method. Comput. Fluids **86**, 28–36 (2013)

13. Greenshields, C.J.: Openfoam User Guide. *OpenFOAM Foundation Ltd, version,* vol. 3, no. 1 (2015)
14. Pooyan, S., Passandideh-Fard, M.: Investigation of the effect of geometric parameters on EWOD actuation in rectangular microchannels. J. Fluids Eng. **140**(9), 091104-091104-9 (2018)
15. Mibus, M., Zangari, G.: Performance and reliability of electrowetting-on-dielectric (EWOD) systems based on Tantalum oxide. ACS Appl. Mater. Interfaces **9**(48), 42278–42286 (2017)
16. Lapierre, F., Jonsson-Niedziolka, M., Coffinier, Y., Boukherroub, R., Thomy, V.: Droplet transport by electrowetting: Lets get rough!. Microfluid. Nanofluid. **15**(3), 327–336 (2013)
17. Murade, C., van den Ende, D., Mugele, F.: Electrically assisted drop sliding on inclined planes. Appl. Phys. Lett. **98**(1), 014102 (2011)
18. Berthier, J.: Micro-drops and Digital Microfluidics. William Andrew, Norwich (2012)